Energy and Photoinduced Electron Transfer in a Wheel-Shaped Artificial Photosynthetic Antenna-Reaction Center Complex

ARTICLE *in* JOURNAL OF THE AMERICAN CHEMICAL SOCIETY · MARCH 2006

Impact Factor: 12.11 · DOI: 10.1021/ja055903c · Source: PubMed

9 AUTHORS, INCLUDING:

Gerdenis Kodis
Arizona State University
75 PUBLICATIONS **2,365** CITATIONS
SEE PROFILE

Joakim Andreasson
Chalmers University of Technology
58 PUBLICATIONS **2,316** CITATIONS
SEE PROFILE

Thomas A Moore
Arizona State University
330 PUBLICATIONS **16,552** CITATIONS
SEE PROFILE

Article

Energy and Photoinduced Electron Transfer in a Wheel-Shaped Artificial Photosynthetic Antenna-Reaction Center Complex

Gerdenis Kodis, Yuichi Terazono, Paul A. Liddell, Joakim Andrasson, Vikas Garg, Michael Hambourger, Thomas A. Moore, Ana L. Moore, and Devens Gust

J. Am. Chem. Soc., **2006**, 128 (6), 1818-1827 • DOI: 10.1021/ja055903c

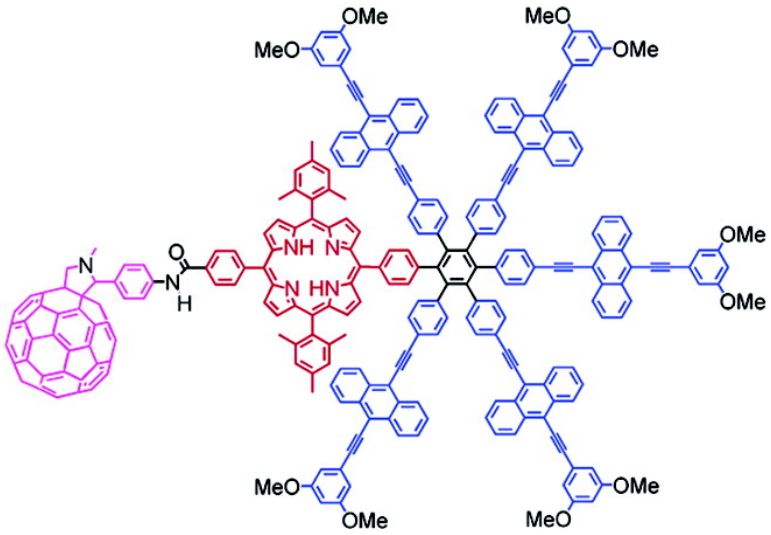

More About This Article

Additional resources and features associated with this article are available within the HTML version:

- Supporting Information
- Links to the 29 articles that cite this article, as of the time of this article download
- Access to high resolution figures
- Links to articles and content related to this article
- Copyright permission to reproduce figures and/or text from this article

View the Full Text HTML

J|A|C|S
ARTICLES
Published on Web 01/24/2006

Energy and Photoinduced Electron Transfer in a Wheel-Shaped Artificial Photosynthetic Antenna-Reaction Center Complex

Gerdenis Kodis, Yuichi Terazono, Paul A. Liddell, Joakim Andréasson, Vikas Garg, Michael Hambourger, Thomas A. Moore,* Ana L. Moore,* and Devens Gust*

Contribution from the Department of Chemistry and Biochemistry, Center for the Study of Early Events in Photosynthesis, Arizona State University, Tempe, Arizona 85287-1604

Received August 26, 2005; Revised Manuscript Received December 9, 2005; E-mail: gust@asu.edu; tom.moore@asu.edu; amoore@asu.edu

Abstract: Functional mimics of a photosynthetic antenna-reaction center complex comprising five bis(phenylethynyl)anthracene antenna moieties and a porphyrin−fullerene dyad organized by a central hexaphenylbenzene core have been prepared and studied spectroscopically. The molecules successfully integrate singlet−singlet energy transfer and photoinduced electron transfer. Energy transfer from the five antennas to the porphyrin occurs on the picosecond time scale with a quantum yield of 1.0. Comparisons with model compounds and theory suggest that the Förster mechanism plays a major role in the extremely rapid energy transfer, which occurs at rates comparable to those seen in some photosynthetic antenna systems. A through-bond, electron exchange mechanism also contributes. The porphyrin first excited singlet state donates an electron to the attached fullerene to yield a $P^{\bullet+}-C_{60}^{\bullet-}$ charge-separated state, which has a lifetime of several nanoseconds. The quantum yield of charge separation based on light absorbed by the antenna chromophores is 80% for the free base molecule and 96% for the zinc analogue.

Introduction

Photosynthetic organisms convert excitation energy from sunlight into electrochemical potential in reaction center pigment−protein complexes. However, most of the light used by an organism is absorbed by antenna systems, and the resulting singlet excitation energy is transferred to the reaction centers. The use of antennas allows organisms to achieve broad coverage of the useful solar spectrum, synthesize fewer reaction centers that can each function at optimal rates, tune the nature and amount of antenna chromophores to adjust to ambient light conditions, and control the amount of light reaching the reaction center in order to reduce harmful photochemical reactions. It is possible to design and synthesize artificial photosynthetic reaction centers that efficiently convert excitation energy into electrochemical potential energy in the form of long-lived charge separation.[1−4] In addition, a variety of antenna mimics based on porphyrins and related chromophores have been studied.[5−23] We have recently reported examples of artificial antenna-reaction center hybrids in which porphyrin antenna chromophores absorb light and transfer the resulting excitation to covalently attached artificial reaction centers that carry out photoinduced electron transfer.[5,6]

Several natural antenna systems consist of cyclic arrays of chromophores such as chlorophylls and carotenoids.[24−27] We

(1) Gust, D.; Moore, T. A. Intramolecular photoinduced electron-transfer reactions of porphyrins. In *The Porphyrin Handbook*; Kadish, K. M., Smith, K. M., Guilard, R., Eds.; Academic Press: New York, 2000; pp 153−190.
(2) Gust, D.; Moore, T. A.; Moore, A. L. *Acc. Chem. Res.* **2001**, *34*, 40−48.
(3) Wasielewski, M. R. *Chem. Rev.* **1992**, *92*, 435−461.
(4) Fukuzumi, S.; Imahori, H. *Electron Transfer in Chemistry* **2001**, *2*, 927−975.
(5) Kodis, G.; Liddell, P. A.; de la Garza, L.; Clausen, P. C.; Lindsey, J. S.; Moore, A. L.; Moore, T. A.; Gust, D. *J. Phys. Chem. A* **2002**, *106*, 2036−2048.
(6) Kuciauskas, D.; Liddell, P. A.; Lin, S.; Johnson, T. E.; Weghorn, S. J.; Lindsey, J. S.; Moore, A. L.; Moore, T. A.; Gust, D. *J. Am. Chem. Soc.* **1999**, *121*, 8604−8614.
(7) Aratani, N.; Osuka, A.; Kim, Y. H.; Jeong, D. H.; Kim, D. *Angew. Chem., Int. Ed.* **2000**, *39*, 1458−1462.
(8) Bothner-By, A. A.; Dadok, J.; Johnson, T. E.; Lindsey, J. S. *J. Phys. Chem.* **1996**, *100*, 17551−17557.
(9) Burrell, A. K.; Officer, D. L.; Plieger, P. G.; Reid, D. C. W. *Chem. Rev.* **2001**, *101*, 2751−2796.
(10) Guldi, D. M. *Chem. Soc. Rev.* **2002**, *31*, 22−36.
(11) Harriman, A. Energy transfer in synthetic porphyrin arrays. In *Supramolecular Photochemistry*; Balzani, V., Ed.; D. Reidel Publishing Company: 1987; pp 207−223.
(12) Li, J.; Ambroise, A.; Yang, S. I.; Diers, J. R.; Seth, J.; Wack, C. R.; Bocian, D. F.; Holten, D.; Lindsey, J. S. *J. Am. Chem. Soc.* **1999**, *121*, 8927−8940.
(13) Li, J.; Diers, J. R.; Seth, J.; Yang, S. I.; Bocian, D. F.; Holten, D.; Lindsey, J. S. *J. Org. Chem.* **1999**, *64*, 9090−9100.
(14) Lin, V. S. Y.; DiMagno, S. G.; Therien, M. J. *Science* **1994**, *264*, 1105−1111.
(15) Nakano, A.; Osuka, A.; Yamazaki, I.; Yamazaki, T.; Nishimura, Y. *Angew. Chem., Int. Ed.* **1998**, *37*, 3023−3027.
(16) Paolesse, R.; Jaquinod, L.; Della Sala, F.; Nurco, D. J.; Prodi, L.; Montalti, M.; Di Natale, C.; D'Amico, A.; Di Carlo, A.; Lugli, P.; Smith, K. M. *J. Am. Chem. Soc.* **2000**, *122*, 11295−11302.
(17) Rucareanu, S.; Mongin, O.; Schuwey, A.; Hoyler, N.; Gossauer, A.; Amrein, W.; Hediger, H.-U. *J. Org. Chem.* **2001**, *66*, 4973−4988.
(18) Cho, H. S.; Rhee, H.; Song, J. K.; Min, C.-K.; Takase, M.; Aratani, N.; Cho, S.; Osuka, A.; Joo, T.; Kim, D. *J. Am. Chem. Soc.* **2003**, *125*, 5849−5860.
(19) Brodard, P.; Matzinger, S.; Vauthey, E.; Mongin, O.; Papamicaël, C.; Gossauer, A. *J. Phys. Chem. A* **1999**, *103*, 5858−5870.
(20) Hwang, I.-W.; Kamada, T.; Ahn, T. K.; Ko, D. M.; Nakamura, T.; Tsuda, A.; Osuka, A.; Kim, D. *J. Am. Chem. Soc.* **2004**, *126*, 16187−16198.
(21) Morandeira, A.; Vauthey, E.; Schuwey, A.; Gossauer, A. *J. Phys. Chem. A* **2004**, *108*, 5741−5751.
(22) Nakamura, Y.; Hwang, I.-W.; Aratani, N.; Ahn, T. K.; Ko, D. M.; Takagi, A.; Kawai, T.; Matsumoto, T.; Kim, D.; Osuka, A. *J. Am. Chem. Soc.* **2005**, *127*, 236−246.
(23) Aratani, N.; Osuka, A.; Cho, H. S.; Kim, D. *J. Photochem. Photobiol., C.* **2002**, *3*, 25−52.

 10.1021/ja055903c CCC: $33.50

Chart 1. Antenna-Reaction Center Heptads

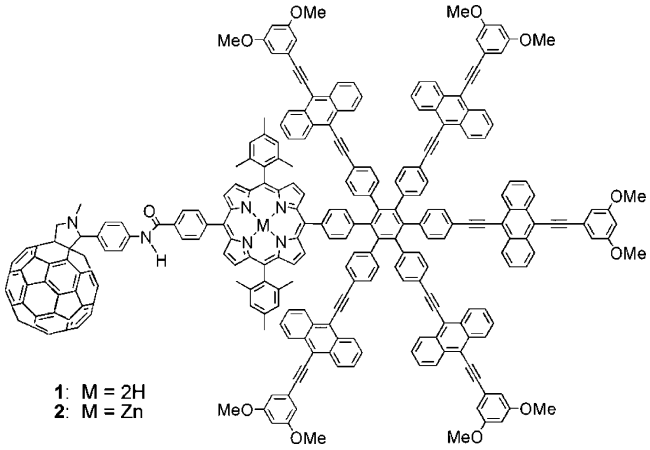

recently reported some initial steps toward the design of artificial cyclic antenna-reaction center complexes based on hexaphenylbenzene as a core that provides structural organization and rigidity.[28] We now report the synthesis and spectroscopic characterization of heptads **1** and **2**, which feature five bis(phenylethynyl)anthracene (BPEA) antennas surrounding a central hexaphenylbenzene core that also bears a porphyrin-fullerene electron donor−acceptor unit (Chart 1). The BPEA antenna chromophore was chosen because it absorbs strongly in the 430 to 475 nm region, where the extinction coefficients of porphyrins and chlorophylls are generally low. In photosynthetic organisms, carotenoid polyenes often serve as antenna chromophores that harvest light in this spectral region. Porphyrin−fullerene systems have been shown to efficiently carry out photoinduced electron transfer to yield charge-separated states with usefully long lifetimes for charge recombination.[29−36] The key to designing a functional antenna-reaction center complex using these building blocks is choosing a molecular architecture that achieves rapid and efficient singlet energy transfer from all of the BPEA antenna moieties to the porphyrin while precluding electronic coupling, energy transfer, or electron-transfer phenomena that interfere with charge separation and recombination within the porphyrin−fullerene unit.

Results

Synthesis. The study required synthesis of not only heptads **1** and **2** but also antenna models **3**−**5** and porphyrin-antenna models **6**−**13** (Charts 2 and 3). The key to the rational synthesis of such unsymmetrical structures based on an inherently symmetric hexaphenylbenzene core was to build up the hexaphenylbenzene using the well-known Diels Alder reaction of tetraphenylcyclopentadienones with diphenylacetylenes. The tetraphenylcyclopentadienones were in turn synthesized by the base-catalyzed reaction of benzils with dibenzyl ketones. We have used this strategy in the past to prepare unsymmetrically substituted hexaphenylbenzenes of well-defined structure.[28,37−39]

Chart 2. Model Compounds

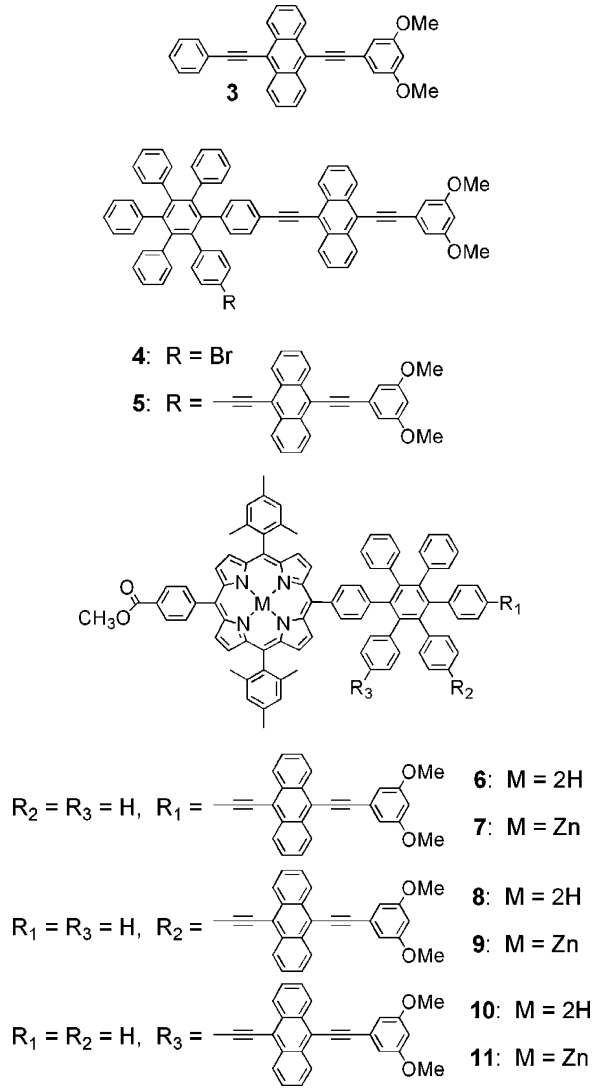

A hexaphenylbenzene core bearing a porphyrin and five bromine atoms, one at the para position of each of five peripheral phenyl rings, was prepared, and the BPEA antennas were coupled to the core using a palladium catalyst. The fullerene was added in the final steps. The details of the synthetic procedures and characterization of the compounds are reported elsewhere.[40]

Bis(diphenylethynyl)anthracene Antennas 3, 4, and 5. The absorption spectra of antenna model compounds **3**−**5** in

(24) Koepke, J.; Hu, X.; Muenke, C.; Schulten, K.; Michel, H. *Structure* **1996**, *4*, 581−597.
(25) McDermott, G.; Prince, S. M.; Freer, A. A.; Hawthornthwaite-Lawless, A. M.; Papiz, M. Z.; Cogdell, R. J.; Isaacs, N. W. *Nature* **1995**, *374*, 517−521.
(26) Fleming, G. R.; van Grondelle, R. *Curr. Opin. Struct. Biol.* **1997**, *7*, 738−748.
(27) Polívka, T.; Sundström, V. *Chem. Rev.* **2004**, *104*, 2021−2071.
(28) Liddell, P. A.; Kodis, G.; de la Garza, L.; Moore, A. L.; Moore, T. A.; Gust, D. *J. Phys. Chem. B* **2004**, *108*, 10256−10265.
(29) Liddell, P. A.; Sumida, J. P.; Macpherson, A. N.; Noss, L.; Seely, G. R.; Clark, K. N.; Moore, A. L.; Moore, T. A.; Gust, D. *Photochem. Photobiol.* **1994**, *60*, 537−541.
(30) Imahori, H.; Hagiwara, K.; Aoki, M.; Akiyama, T.; Taniguchi, S.; Okada, T.; Shirakawa, M.; Sakata, Y. *J. Am. Chem. Soc.* **1996**, *118*, 11771−11782.
(31) Imahori, H.; Hagiwara, K.; Akiyama, T.; Aoki, M.; Taniguchi, S.; Okada, T.; Shirakawa, M.; Sakata, Y. *Chem. Phys. Lett.* **1996**, *263*, 545−550.
(32) Guldi, D. M.; Torres-Garcia, G.; Mattay, J. *J. Phys. Chem. A* **1998**, *102*, 9679−9685.
(33) Schuster, D. I. *Carbon* **2000**, *38*, 1607−1614.
(34) Bahr, J. L.; Kuciauskas, D.; Liddell, P. A.; Moore, A. L.; Moore, T. A.; Gust, D. *Photochem. Photobiol.* **2000**, *72*, 598−611.
(35) Liddell, P. A.; Kuciauskas, D.; Sumida, J. P.; Nash, B.; Nguyen, D.; Moore, A. L.; Moore, T. A.; Gust, D. *J. Am. Chem. Soc.* **1997**, *119*, 1400−1405.
(36) Kuciauskas, D.; Liddell, P. A.; Lin, S.; Stone, S.; Moore, A. L.; Moore, T. A.; Gust, D. *J. Phys. Chem. B* **2000**, *104*, 4307−4321.
(37) Gust, D. *J. Am. Chem. Soc.* **1977**, *99*, 6980−6982.
(38) Gust, D.; Fagan, M. W. *J. Org. Chem.* **1980**, *45*, 2511−2512.
(39) Patton, A.; Dirks, J. W.; Gust, D. *J. Org. Chem.* **1979**, *44*, 4749−4752.
(40) Terazono, Y.; Liddell, P. A.; Garg, V.; Kodis, G.; Brune, A.; Hambourger, M.; Moore, T. A.; Moore, A. L.; Gust, D. *J. Porphyrins Phthalocyanines* **2005**, in press.

Chart 3. Model Hexad Antenna System

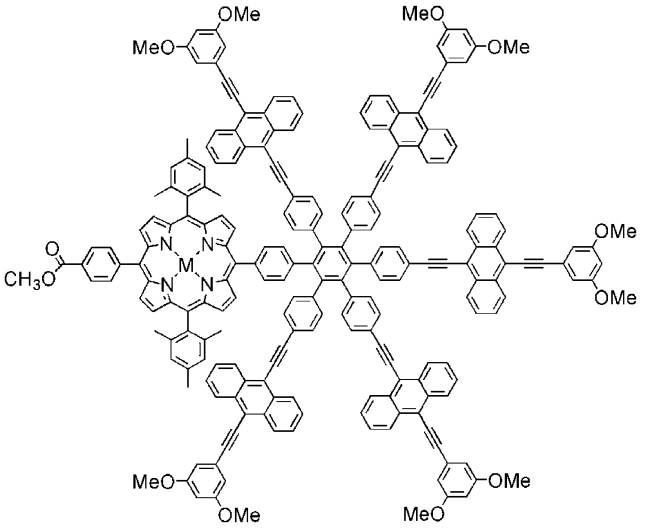

12: M = 2H
13: M = Zn

2-methyltetrahydrofuran are shown in Figure 1a. BPEA **3** features maxima at 311, 439, and 457 nm. Attachment to the hexaphenylbenzene core (molecule **4**) results in the appearance of two bands in the UV region at 309 and 319 nm and a ca. 10 nm shift of the visible bands to longer wavelengths (445 and 469 nm). Thus, the hexaphenylbenzene core influences the electronic structure of the BPEA, even though $\pi-\pi$ interactions between the BPEA and the central benzene ring are limited due to the 65°−90° dihedral angle between the two directly bonded rings.[41−43] Addition of a second BPEA to the hexaphenylbenzene core at an ortho position, as in the case of **5**, increases the extinction coefficient of the bands in the visible and changes the relative band intensities slightly but does not significantly shift the positions of the band maxima, which appear at 309, 319, 444, and 468 nm (Figure 1a). Thus, the BPEA chromophores do not interact strongly by excitonic or other mechanisms. The long-wavelength absorption band of hexaphenylbenzene itself is observed at ca. 275 nm.

Figure 1b shows the fluorescence emission spectra of **3**−**5** obtained with excitation at 400 nm. The emission band positions of **4** and **5** are nearly identical (483, 515, and ca. 547 (sh.) nm) and are shifted about 10 nm to longer wavelengths than those of **3** (474, 505, and ca. 536 (sh.) nm). Thus, the emission spectral changes parallel those noted in absorption and show no evidence for strong electronic interactions between adjacent BPEA moieties on the central core. The fluorescence quantum yield of **4** was determined to be 0.94, using the comparative method with Rhodamine 6G as the standard ($\Phi = 0.90$ in water[44]). The energy of the BPEA excited state in **4** is calculated to be 2.61 eV from the wavenumber average of the long-wavelength absorption maximum and the short-wavelength emission maximum.

Time-resolved fluorescence studies of **4** and **5** were undertaken using the single photon timing method. Excitation was at

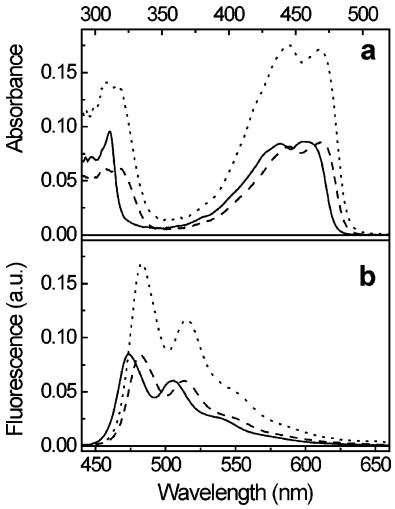

Figure 1. Absorption (a) and emission (b) spectra of model antennas **3** (—), **4** (− −), and **5** (- - -).

300 nm in 2-methyltetrahydrofuran. Emission from compound **4** was measured at 480 nm and found to decay as a single-exponential process with a lifetime of 2.80 ns ($\chi^2 = 1.19$). A similar experiment with **5** gave a lifetime of 2.83 ns ($\chi^2 = 1.06$).

Given the close spatial arrangement of the BPEA chromophores in **1** and **2**, singlet−singlet energy transfer between them is a reasonable possibility. To investigate this question, the decay of the polarization anisotropy of fluorescence and stimulated emission were studied in model antennas **4** and **5**. In this experiment, the sample is excited with a plane-polarized laser pulse, and fluorescence intensities parallel (I_{VV}) and perpendicular (I_{VH}) to the pulse polarization are measured as a function of time. At a given time, the fluorescence polarization anisotropy r is given by eq 1, where G is an instrumental correction factor. The value of r will be maximal if the absorbing and emitting transition dipoles are parallel.

$$r(t) = \frac{I_{VV}(t) - GI_{VH}}{I_{VV}(t) + 2GI_{VH}(t)} \tag{1}$$

The anisotropy can decay as a function of time after the pulse due to rotation of the transition dipole (via tumbling of the molecule in solution or internal motions) or due to energy transfer to a second chromophore (whose transition dipole is not parallel to that of the donor), which then emits.

The fluorescence anisotropy decay at 510 nm for antenna **4** following excitation at 300 nm was measured in 2-methyltetrahydrofuran solution using the single photon timing method. The result was a single exponential with a time constant of 440 ps. Because intermolecular singlet energy transfer between molecules of **4** is slow in the dilute solution employed, and internal motions are limited, this time constant is associated with the rotation of **4** in solution. Equation 2, where r_0 is the initial value of r and ϕ is the orientational relaxation time, describes this situation.[45]

$$r(t) = r_0 e^{-t/\phi} \tag{2}$$

Thus, the reorientation time of **4** is 440 ps. The reorientation time of a spherical rotor molecule may be estimated using the

(41) Almenningen, A.; Bastiansen, O.; Skancke, P. N. *Acta Chemica Scandinavica* **1958**, *12*, 1215−1220.
(42) Bart, J. C. J. *Acta Crystallogr., Sect. B* **1968**, *24*, 1277−1287.
(43) Larson, E. M.; Von Dreele, R. B.; Hanson, P.; Gust, D. *Acta Crystallogr.* **1990**, *C46*, 784−788.
(44) Magde, D.; Wong, R.; Seybold, P. G. *Photochem. Photobiol.* **2002**, *75*, 327−334.

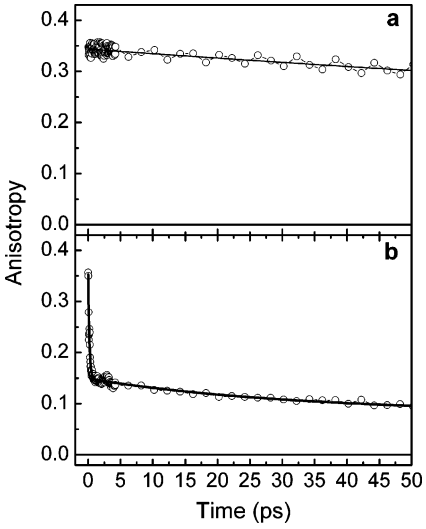

Figure 2. (a) Stimulated emission anisotropy decay of **4** measured at 500 nm with excitation at 450 nm. The solid line is an exponential fit with $\tau = 440$ ps. (b) Stimulated emission anisotropy decay of **5** measured at 500 nm with excitation at 450 nm. The solid line is a three-exponential fit with $\tau = 0.2$, 30, and 560 ps.

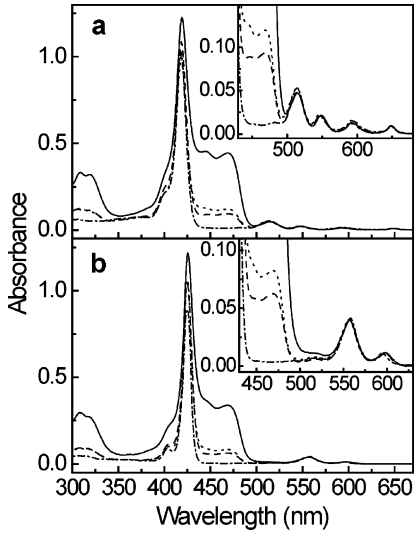

Figure 3. Absorption spectra of (a) **12** (—), **6** (- - -), **10** (— — —), and model free base porphyrin **14** (— - — - —) and (b) **13** (—), **7** (- - -), **11** (— — —), and model zinc porphyrin **15** (— - — - —) in 2-methyltetrahydrofuran.

Debye−Stokes−Einstein equation[46] (eq 3), where η is the viscosity of the solvent, k_B is the Boltzmann constant, and V is the volume of the sphere.

$$\phi = \eta V/k_B T \tag{3}$$

Using the crude approximation that **4** is a sphere with a radius of 12.5 Å (based on molecular models), eq 3 yields a value of $\phi = 970$ ps, which is in reasonable agreement with the measured reorientation time, given the approximations involved. Although internal motions of **4** that would affect ϕ are expected to be slow, given the rigidity of the framework, the molecule is certainly not an isotropic rotor.

Turning now to dyad **5**, the fluorescence anisotropy decay was found to be biexponential, with time constants of 560 and 40 ps. The 560 ps lifetime is ascribed to overall tumbling of the molecule. We also employed transient absorption methods in order to increase the time resolution of the anisotropy measurements. Figure 2a shows the stimulated emission anisotropy decay of **4** at 500 nm following laser pulse excitation at 450 nm. The data were fitted with a time constant of 440 ps. Figure 2b gives the stimulated emission anisotropy decay of **5** at 500 nm. Exponential fitting of the data yielded three components with lifetimes of 0.20 (58%), 30 (15%), and 560 (27%) ps. The longest lifetime is not well defined in the time window available and was, therefore, fixed at the same value as that obtained in the single photon timing experiments. For each molecule, the long component, 440 or 560 ps, is assigned to rotational diffusion. The short component for **5** is associated with degenerate singlet−singlet energy transfer between the two BPEA moieties. Given that the anisotropy decays with a rate constant twice that of energy transfer, the time constant for excitation exchange between adjacent BPEA moieties is 0.40 ps. A minor component (30 ps) makes up 15% of the decay. It is likely that this component is due to the presence of rotational isomers of BPEA that differ in the orientation of the anthracene ring system relative to the appended phenyl rings. Calculations and spectroscopic studies on BPEA itself reveal that although the conformation with all three ring systems coplanar is most stable, a conformation with the anthracene ring perpendicular to the other two is also populated.[47] The oscillator strength of the minor conformer is 35% smaller than that for the major conformer. To the extent that a similar conformational heterogeneity also appears in **5**, the minor conformation would be a less effective energy acceptor and donor by the Förster mechanism (vide infra), and the energy transfer time constant would be larger. Alternatively, the minor component could be ascribed to an impurity, but none was detected by the usual chromatographic, NMR, and mass spectral analyses.

BPEA−Porphyrin Dyads 6−11. Having obtained the rate constant for singlet−singlet energy transfer between adjacent BPEA moieties, we next determined energy transfer rates from a BPEA directly to a free base or zinc porphyrin located ortho, meta, or para to it on the central ring of the hexaphenylbenzene. This information was obtained from dyads **6**−**11**. Figure 3 shows the absorption spectra of these dyads, those of hexads **12** and **13**, and those of model porphyrins 5-(4-carbomethoxyphenyl)-10,15,20-tris(2,4,6-trimethylphenyl)porphyrin (**14**) and zinc 5,10,15,20-tetrakis(2,4,6-trimethylphenyl)porphyrin (**15**). The spectra have been normalized in the porphyrin Q-band region where the BPEA does not absorb. The spectra of **8** and **9** are virtually identical to those of **6** and **7**, respectively, and have not been shown. The spectral shapes and absorption maxima of the bands in the dyads are essentially identical to a linear combination of those of the corresponding model BPEA and porphyrins. No large shifts or perturbations occur as a result of covalently linking the chromophores. The amplitude of the BPEA absorption (430−500 nm region) in ortho-linked **10** and **11** is slightly reduced, compared to those in the dyads in which the chromophores are in the meta and para relationships. Overall, these results indicate that any electronic interaction between

(45) Gustavsson, T.; Cassara, L.; Marguet, S.; Gurzadyan, G.; van der Meulen, P.; Pommeret, S.; Mialocq, J.-C. *Photochem. Photobiol. Sci.* **2003**, *2*, 329−341.
(46) Debye, P. *Polar Molecules*; Chemical Catalog Company: New York, 1929.
(47) Levitus, M.; Garcia-Garibay, M. A. *J. Phys. Chem. A* **2000**, *104*, 8632−8637.

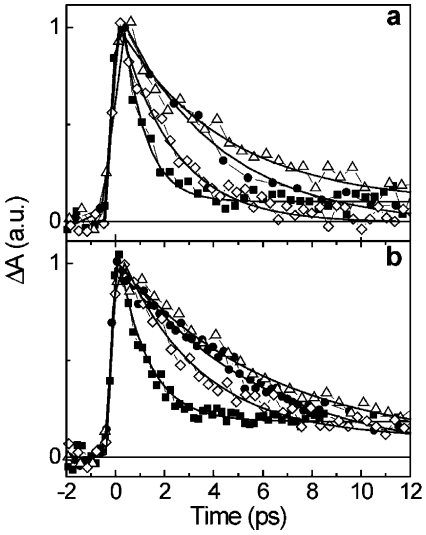

Figure 4. (a) Transient absorption kinetics of free base compounds at 650 nm with 480 nm excitation: **6** (●), **8** (△), **10** (■), **12** (◇). (b) Transient absorption kinetics of zinc compounds at 600 nm with 480 nm excitation: **7** (●), **9** (△), **11** (■), **13** (◇).

BPEA and porphyrin moieties is weak enough that the various chromophores may be considered as individual but interacting chromophores, rather than a single extended chromophore or a strongly excitonically coupled system.

Excitation of either the BPEA or the free base porphyrin moieties of dyads **6**, **8**, and **10** results in typical porphyrin fluorescence with maxima at 651 and 720 nm. This suggests significant singlet−singlet energy transfer from the BPEA to the porphyrin. A very small amount of residual fluorescence from the BPEA is also observed. From the absorption and emission data, the first excited singlet state of the porphyrin in the free base dyads is estimated to lie 1.91 eV above the ground state. For zinc dyads **7**, **9**, and **11**, fluorescence maxima are at 603 and 655 nm, as is typical for zinc porphyrins. In this case, the porphyrin excited-state energy is 2.07 eV.

The fact that excitation of the BPEA moieties of the dyads results in fluorescence emission almost exclusively from the porphyrin suggests that the efficiencies of singlet−singlet energy transfer are high in all of the compounds. Transient absorption pump−probe experiments were undertaken in order to learn more about this process. The BPEA moieties of the various molecules in 2-methyltetrahydrofuran were excited with 100 fs laser pulses at 480 nm, and the decay of the transient absorbance was monitored over the 490−760 nm spectral region. The complete data set was fitted by a global analysis procedure. This procedure is described in the Supporting Information. Random errors associated with the reported lifetimes obtained from fluorescence and transient absorption measurements were typically <10%. The results are illustrated in Figure 4, along with some representative decays. For free base dyad **6**, with the para relationship between the chromophores, the decay was best fitted with two exponential components with time constants of 4.0 ps and 10 ns (solid line in Figure 4a). The solution of dyad **8**, with the meta relationship, contained 25% of **6**, as the two materials could not be completely separated. The decay was fitted by analysis at several wavelengths with three time constants: 4.0 ps (fixed using the results from **6**), 8.0 ps, and 10 ns. For dyad **10**, in which the chromophores are in the ortho relationship, the time constants from global analysis were 0.9 ps and 10 ns. In each case, the 10-ns component is taken as the time constant for decay of the porphyrin first excited singlet state and is essentially the same as that for the relevant porphyrin model system.

The pattern of decays was similar for the zinc analogues (Figure 4b). Two-exponential fits were required. The longer component for dyads **7**, **9**, and **11** was 2.4 ns, which is similar to the lifetime of the excited state of the zinc porphyrin model system. The shorter components were 5.7 ps, 7.0 ps (obtained from a three-exponential fit as described for **8**), and 1.2 ps for the para (**7**), meta (**9**), and ortho (**11**) isomers.

Because the lifetime of the first excited singlet state of BPEA in **4** and **5** is 2.8 ns, the very rapid decays of the transient absorbance attributed to these moieties are taken to reflect singlet−singlet energy transfer to the porphyrin. This is verified by the fact that transient absorption features characteristic of the porphyrin first excited singlet states grew in with the same time constants. Another conceivable quenching mechanism, photoinduced electron transfer, is thermodynamically precluded for these compounds (vide infra). This being the case, the rate constant for singlet−singlet energy transfer, k_{ent}, is given by eq 4,

$$k_{ent} = (1/\tau) - k_s \qquad (4)$$

where τ is the experimentally observed decay time for BPEA fluorescence and k_s is the rate constant for decay of the BPEA excited state by all processes other than energy transfer. Taking k_s as 3.6×10^8 s^{-1} (from the 2.80 ns lifetime of **4**) and the τ values listed above, singlet−singlet energy transfer rate constants of 2.5×10^{11}, 1.3×10^{11}, and 1.1×10^{12} s^{-1} were calculated for free base dyads **6**, **8**, and **10**, respectively. For the zinc series, the rate constants were 1.8×10^{11}, 1.4×10^{11}, and 8.3×10^{11} s^{-1}, respectively. Energy transfer is faster in the free base series than in the zinc series. Transfer from BPEA to an ortho porphyrin is faster than transfer to a para porphyrin in each series, and transfer to a porphyrin with a meta relationship is slowest in both series.

Hexads 12 and 13. The absorption spectrum of free base hexad **12** is shown in Figure 3a. The bands associated with the porphyrin moiety are essentially unchanged from their positions in the model porphyrin **14** and the various dyads. The BPEA portion of the spectrum has maxima at 445 and 469 nm, in common with the dyads. The extinction coefficient at 469 nm is approximately the sum of those of two ortho, two meta, and one para BPEA in the model compounds. Thus, introducing five BPEA moieties on the hexaphenylbenzene core does not significantly perturb the spectra of the individual chromophores. The fluorescence spectrum of the hexad has porphyrin maxima at 652 and 721 nm, which are similar to those for dyads **6**, **8**, and **10**. A small amount of BPEA emission is observed as well. Time-resolved fluorescence studies of **12** using the single photon timing method with excitation at 300 nm yielded a decay at 720 nm that was fitted by a single exponential ($\chi^2 = 1.10$) with a time constant of 10.3 ns, which is essentially identical to that of the model porphyrin. Emission from BPEA at 510 nm following excitation at 300 nm had a lifetime of <10 ps ($\chi^2 = 1.20$), which is near the time resolution limit of the spectrometer. This is consistent with rapid energy transfer from all of the BPEA moieties to the porphyrin.

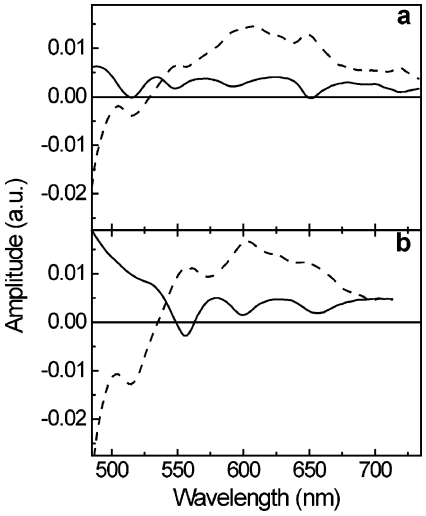

Figure 5. (a) Transient absorption decay-associated spectra of hexad **12** with excitation at 480 nm. Two components with time constants of 2.2 ps (− − −) and nondecaying (—) were observed. (b) Similar decay-associated spectra for zinc analogue **13**. The two components have time constants of 3.2 ps (− − −) and 2.4 ns (—).

Increased time resolution was achieved using the pump−probe transient absorption technique. Figure 5a shows the decay-associated spectra obtained after excitation of the BPEA moieties of **12** at 480 nm with a 100 fs laser pulse. Two kinetic components, ca. 2.2 ps and nondecaying on this time scale, were observed. The long-lived component shows characteristic porphyrin transient absorption, ground-state bleaching, and stimulated emission bands and is ascribed to the decay of the porphyrin first excited singlet state (10.3 ns based on the fluorescence results). The short component features decay of BPEA stimulated emission below 530 nm and decay of BPEA induced absorption and grow-in of porphyrin stimulated emission at longer wavelengths. Thus, this component is associated with singlet−singlet energy transfer from the BPEA to porphyrin. Figure 4a shows the kinetic trace at 650 nm and a fit with two exponential components of 2.2 ps and 10 ns. These results indicate that all of the energy transfer processes are complete with time constants of about 2 ps. Given that the BPEA model chromophore has an excited state lifetime of 2.8 ns, the rapid decay of the BPEA excited states in the hexad suggests that the energy transfer quantum yield should be essentially unity.

Energy transfer was also investigated in zinc hexad **13**. The absorption spectrum of **13** is shown in Figure 3b. The bands associated with the porphyrin moiety are essentially unchanged from their positions in the model porphyrin **15** and the dyads. The BPEA portion of the spectrum has maxima at 445 and 469 nm, in common with those of the dyads, and the extinction coefficient at 469 nm is approximately the sum of those of two ortho, two meta, and one para BPEA in the model compounds. The fluorescence spectrum of the hexad has porphyrin maxima at 605 and 656 nm, which are similar to those for **7**, **9**, and **11**. Time-resolved fluorescence studies of **13** with excitation at 300 nm yielded a single-exponential decay at 650 nm ($\chi^2 = 1.14$) with a time constant of 2.35 ns, which is essentially identical to that of the model zinc porphyrin. Emission from BPEA at 510 nm following excitation at 300 nm had a lifetime of <10 ps ($\chi^2 = 1.19$), as was observed for the free base analogue.

The pump−probe transient absorption technique was again employed to achieve increased time resolution. Figure 4b shows

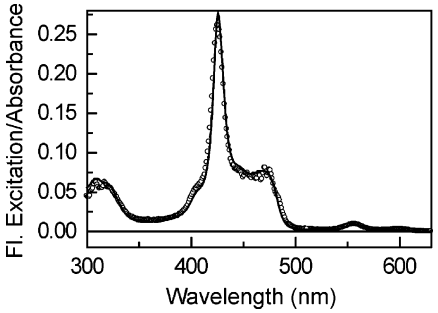

Figure 6. Steady-state absorption (—) and corrected fluorescence excitation (○) spectra of zinc hexad **13**. Fluorescence was monitored at 650 nm.

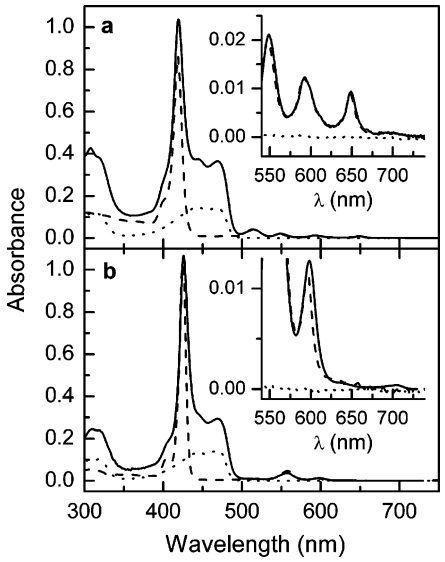

Figure 7. Absorption spectra of (a) **1** (—), **5** (- - - -), and a model porphyrin−fullerene dyad (− − −) and of (b) **2** (—), **5** (- - - -), and a model porphyrin **15** (− − −) in 2-methyltetrahydrofuran.

the transient absorbance decay at 600 nm obtained after excitation of the BPEA moieties. Two kinetic components of ~3.2 ps and 2.4 ns were observed. The first is the decay of BPEA excitation due to energy transfer to the porphyrin, and the second is due to decay of the zinc porphyrin first excited singlet state by the usual photophysical pathways (see Figure 5b). Thus, singlet−singlet energy transfer occurs in **13** with an efficiency close to 100%, as was the case with the free base hexad.

Singlet−singlet energy transfer in **12** and **13** was also evaluated using steady-state fluorescence excitation spectroscopy. In this experiment, the porphyrin fluorescence was monitored as a function of the wavelength of the exciting light. The excitation spectrum was corrected for variations in excitation light intensity with wavelength. The results for **13** are shown in Figure 6. It is clear that the excitation and absorption spectra, normalized in a region where only the porphyrin absorbs, are nearly identical. This is even true in the 440−490 nm region where absorption is due to the BPEA moiety. This experiment verifies that singlet−singlet energy transfer in **13** has a quantum yield of nearly 100%. Similar results, with a transfer efficiency of 100%, were obtained for hexad **12**.

Heptad Reaction Center Models 1 and 2. The absorption spectrum of free base heptad **1** is shown in Figure 7a, along with those of BPEA model **5** and a model for the porphyrin−fullerene portion of the molecule.[48] The fullerene has very weak

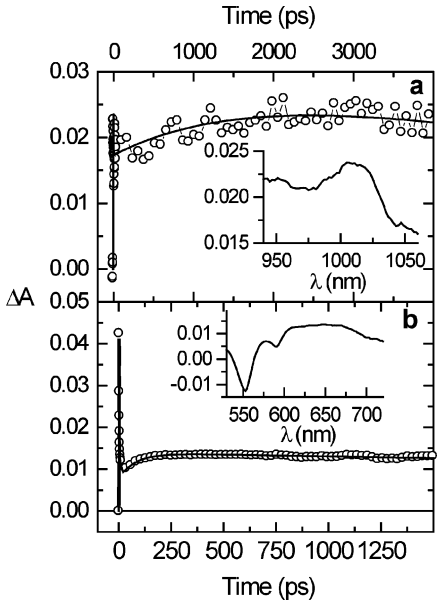

Figure 8. Transient absorption data for heptads **1** and **2** with excitation at 480 nm. (a) Kinetics at 1000 nm for free base heptad **1**. The solid line is a fit to exponentials with time constants of 2.2 ps, 2.0 ns, and 8 ns. The inset shows the transient absorption spectrum 3.0 ns after excitation. (b) Kinetics at 650 nm for zinc heptad **2**. The solid line is a fit to exponentials with time constants of 3.2 ps, 80 ps, and 15 ns. The inset shows the transient absorption spectrum 500 ps after excitation.

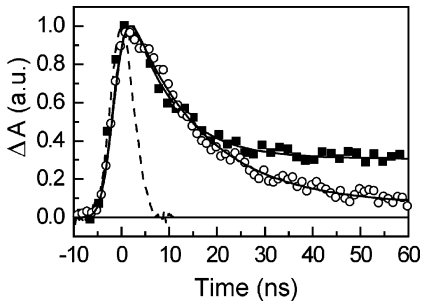

Figure 9. Nanosecond transient absorption kinetics at 1000 nm for heptads **1** (■) and **2** (○) with excitation at 480 nm. By reconvolution with the 4.8 ns instrument response function (− − −) the data for each molecule were fitted with two exponential decays (—). For free base **1**, a time constant of 8.9 ns and a component that did not decay in this time window were obtained. For **2**, a time constant of 15.3 ns and a nondecaying component were detected.

absorption throughout the visible and a small maximum at 704 nm. As was the case with the model compounds, the spectrum of the heptad is essentially a linear combination of the spectra of the individual model chromophores. The heptad has porphyrin fluorescence maxima at 652 and 720 nm, as is the case with the other free base porphyrins studied here, but the fluorescence is quenched relative to that of hexad **12**. The absorption spectrum of zinc porphyrin heptad **2** is shown in Figure 7b, along with those of BPEA model **5** and a model porphyrin **15**. The spectrum of the heptad is essentially a linear combination of the spectra of the individual model chromophores. The heptad has porphyrin fluorescence maxima at 605 and 655 nm, as is the case with the other zinc porphyrins studied here, but the fluorescence is quenched relative to that of hexad **13**.

The nature of the porphyrin quenching was investigated using transient absorption techniques (Figure 8). Excitation was into the BPEA moieties at 480 nm using a 100 fs laser pulse. A spectrum taken 3.0 ns after excitation (inset, Figure 8a) shows an absorbance at ca. 1015 nm that is characteristic of the fullerene radical anion.[48] The kinetic trace at 1000 nm shows that this species forms with a time constant of 2.0 ns and has a long lifetime on the time scale of the experiment. The formation of the fullerene radical anion is ascribed to photoinduced electron transfer from the porphyrin first excited singlet state to yield the porphyrin radical cation and the fullerene radical anion. The formation time is identical to that observed for the $P^{\bullet+}-C_{60}^{\bullet-}$ state from a porphyrin−fullerene dyad having a very similar structure.[48] For zinc heptad **2**, a kinetic trace taken at 650 nm (see Figure 8b) shows very fast decay of the excited states of the antenna chromophores and at later times a rise of transient absorbance whose spectrum is characteristic of the zinc porphyrin radical cation. This species forms with a time constant of 80 ps and has a long lifetime on the time scale of the experiment. The formation of the zinc porphyrin radical cation is ascribed to photoinduced electron transfer from the porphyrin first excited singlet state to the fullerene to yield the corresponding charge-separated state. Single-photon-timing fluorescence measurements confirmed an 80-ps lifetime for the zinc porphyrin first excited singlet state in **2**.

Figure 8 verifies the formation of $P^{\bullet+}-C_{60}^{\bullet-}$ charge-separated states in **1** and **2**, but we turned to nanosecond time-resolved spectroscopy in order to determine the lifetimes of those states. Figure 9 shows the transient absorption kinetics at 1000 nm, which reflect the fullerene radical anion. After deconvolution from the instrument response, the data for **1** could be fitted as two decays, one with a time constant of 8.9 ns and one that did not decay on the time scale shown. The first lifetime is associated with decay of $P^{\bullet+}-C_{60}^{\bullet-}$ (and the band at 1015 nm), and the second with triplet states. The decay was monitored for a total of 2 μs, and the decay time constant for the long component was found to be reduced when oxygen was admitted to the sample, thus verifying the assignment of this component to triplet states. Consistent with this assignment, the spectra in the 900−1010 nm region were essentially structureless. The triplet forms at least in part by intersystem crossing from the porphyrin first excited singlet state, as the time constant for decay of the singlet is relatively long. For heptad **2**, the charge-separated state decayed with a lifetime of 15.3 ns. In this case, a smaller amount of long-lived transient absorbance, ascribed to triplet states, was observed. Although spectroscopic evidence for generation of triplet in **1** and **2** by charge recombination was not observed, at least some triplet formation by this pathway cannot be excluded.

Discussion

It is clear from the results that excitation of any of the BPEA antenna moieties of heptads **1** or **2** results in transfer of singlet excitation energy to the porphyrin with a quantum yield near unity and that this excitation drives photoinduced electron transfer to produce a charge-separated state. By comparing the spectroscopic results for the heptads with those for the various model compounds, it is possible to derive rate constants and quantum yields for the various processes of interest, as described below. The processes of interest are indicated in Figure 10, and the results are reported in Table 1.

(48) Straight, S. D.; Andréasson, J.; Kodis, G.; Moore, A. L.; Moore, T. A.; Gust, D. *J. Am. Chem. Soc.* **2005**, *127*, 2717−2724.

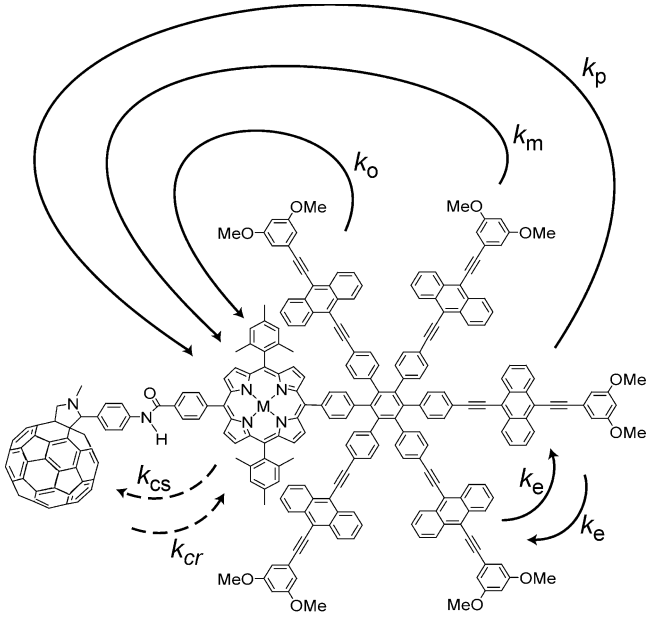

Figure 10. Diagram identifying rate constants for the various energy and electron-transfer processes in the heptads.

Table 1. Energy and Electron Transfer Rate Constants

	heptad **1**		heptad **2**	
rate constant (s^{-1})	expt	calcd	expt	calcd
k_e	2.5×10^{12}	1.9×10^{12}	2.5×10^{12}	1.9×10^{12}
k_o	1.1×10^{12}	3.8×10^{12}[a] 1.3×10^{12}[a]	8.3×10^{11}	2.3×10^{12}
k_m	1.3×10^{11}	1.9×10^{11}[a] 8.8×10^{10}[a]	1.4×10^{11}	1.3×10^{11}
k_p	2.5×10^{11}	7.4×10^{10}	1.8×10^{11}	6.7×10^{10}
k_{cs}	4.0×10^{8}		1.2×10^{10}	
k_{cr}	1.1×10^{8}		6.5×10^{7}	

[a] Values are reported for the two isomers that differ in the disposition of hydrogen atoms on the porphyrin nitrogen atoms, as discussed in the text.

Antenna Function. The steady-state spectroscopic results for all of the compounds and the time-resolved studies on the models show that although the seven chromophores are covalently linked in the heptads, they retain their individual photophysical properties and are not strongly perturbed by their neighbors. The absorption and emission spectra are little changed, and the excited-state lifetimes of the BPEA moieties in **5** and of the porphyrins in **6**−**13** are the same as those in monomeric model chromophores. Strong excitonic interactions are not observed, even though the chromophores are in close proximity. Given this situation, we first make the assumption that energy transfer rate constants in the heptads are, within experimental error, identical to those measured for the corresponding processes in the various model compounds. Using this assumption, the rate constants shown for the various processes in Figure 10 have been estimated as those in Table 1. To test this assumption, we have simulated the decay of the BPEA excited-state transient absorption (rise of the porphyrin transient) expected after random excitation of the five BPEA antennas of **12** and **13**, using the Chemical Kinetics Simulator from IBM Corporation. Processes represented by k_e, k_o, k_m, and k_p were employed. The results are shown in Figure 11. The simulated decays (smooth curves) agree reasonably well with the experimental data, although the simulated curves decay slightly more rapidly than the data. This deviation may reflect small conformational or electronic effects in the hexads that are not well represented by the model compounds. For example, it was noted above that the extinction coefficient of a BPEA unit ortho to the porphyrin is reduced (by ~25%, Figure 3), relative to that of the other BPEA units, presumably including those in model dyad **5**. If singlet energy transfer in the heptads from a BPEA meta to the porphyrin to one ortho to the porphyrin occurs by the Förster mechanism (vide infra), such a reduction would decrease the rate of energy transfer between these BPEA units proportionately, and this would help explain the discrepancy. In addition, the fact that the refractive index for some transfer processes (eq 5) differs for the hexad and the model compounds may play a role.[49]

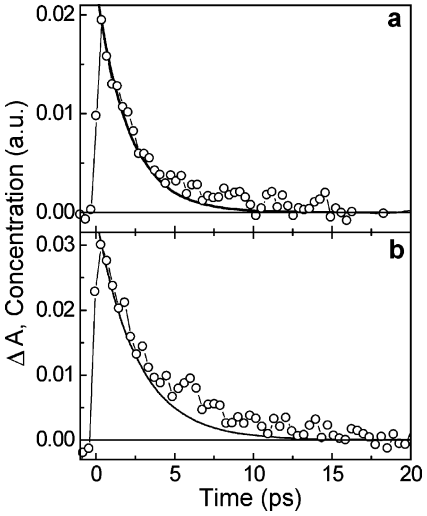

Figure 11. Experimental transient absorption decay of the BPEA moieties of free base hexad **12** (a) and zinc hexad **13** (b) measured at 650 and 600 nm, respectively. Decays simulated using the rate constants in Table 1 appear as smooth curves.

In the simplest theoretical formalism, there are two components to the singlet−singlet energy transfer process. At one extreme, transfer is described by the Förster dipole−dipole mechanism[50,51] which is Coulombic in nature, and at the other extreme, transfer occurs by the Dexter electron-exchange mechanism,[52] which requires significant orbital overlap.

In most cases, the Förster mechanism dominates singlet−singlet energy transfer. The theoretical transfer rate, k_{DD}, may be calculated using Förster's eq 5,

$$k_{DD} = \frac{0.529\kappa^2\Phi_{f(D)}}{n^4 N \tau_D R^6}\int f_D(\nu)\epsilon_A(\nu)\nu^{-4}\,d\nu \qquad (5)$$

where κ is an orientation factor, $\Phi_{f(D)}$ is the fluorescence quantum yield of the donor chromophore, n is the index of refraction of the medium, N is Avogadro's number, τ_D is the lifetime of the donor first excited singlet state in the absence of energy transfer, R is the separation of the dipoles, and ν is the frequency. The integral is the overlap of the normalized donor fluorescence emission spectrum with the absorbance spectrum

(49) Knox, R. S.; van Amerongen, H. *J. Phys. Chem. B* **2002**, *106*, 5289−5293.
(50) Förster, T. *Annalen der Physik* **1948**, *2*, 55−75.
(51) Förster, T. *Discuss. Faraday Soc.* **1959**, *27*, 7−17.
(52) Dexter, D. L. *J. Chem. Phys.* **1953**, *21*, 836−850.

of the acceptor. Hexads **12** and **13** are conformationally restricted due to the aromatic rings and the steric interactions between them. The most stable conformation was estimated using molecular mechanics methods (MM2), and relevant distances and angles taken from the results were used to estimate R and κ. The relevant spectroscopic parameters were estimated from those of model compounds, and the Förster energy transfer rate constants were calculated. They are listed in Table 1.

The lowest-energy transition for BPEA is polarized along the long axis of the chromophore.[47] The porphyrin Q-band region, which is associated with the energy-accepting transitions for transfer from BPEA, consists of two transition moments, each lying along an axis passing through two opposite nitrogen atoms. The molecular mechanics calculations for the heptads indicate that the porphyrin plane is essentially coplanar with the plane of the central benzene ring of the hexaphenylbenzene core. This geometry is enforced by the steric interactions between the porphyrin meso aromatic ring attached to the core and the β-pyrrole hydrogens on one hand and the ortho-aryl rings of the hexaphenylbenzene core on the other. Rotations about the bonds joining this meso ring to the porphyrin macrocycle and the core are very slow on the time scale of energy transfer.[37,40,53,54] Thus, each Q-band transition will have a different value for κ. To obtain each BPEA−porphyrin energy transfer rate constant in Table 1, the rate constants calculated for the two orthogonal Q-band transitions have been summed.

Exchange of the central nitrogen-bound protons in free base porphyrins is slow on the time scale of singlet energy transfer.[55] Therefore, for the free base ortho and meta model compounds, there are actually two essentially isoenergetic populations of molecules that differ in the orientation of the protonated nitrogen atoms of the porphyrin and, therefore, in the orientation of the Q_x and Q_y transition dipoles relative to the BPEA antenna. The two populations have different values of κ for each transition and, therefore, different energy transfer rate constants. Both calculated rate constants are reported in Table 1.

For excitation exchange between adjacent BPEA groups, the calculated rate constant is comparable to the experimental number for model compound **5**. Förster type transfer thus appears to be a viable mechanism for this exchange, although the simple theory is not strictly applicable to systems such as these where chromophore dimensions and separations are comparable.[56] Calculated rate constants for energy transfer from BPEA units to zinc or free base porphyrin moieties at ortho, meta, or para positions on the hexaphenylbenzene core are also in reasonable agreement with experimental values for the model dyads (within a factor of ~3 in all cases). Although two populations of porphyrins with different orientations of the central protons are expected in the ortho and meta compounds, as discussed above, the rate constants calculated for both populations are similar and would not be distinguished experimentally, given the signal-to-noise level in the data.

Given the relatively good agreement between the experimental and calculated rate constants for energy transfer, we used the Förster theory to calculate rate constants for energy transfer between BPEA units meta or para to one another on the hexaphenylbenzene core. The rates obtained were much too slow to compete with the other energy transfer processes discussed above, and we conclude that such transfers do not contribute significantly to the photochemistry of the hexads.

Despite the relatively good agreement between experimental results and Förster theory, the Dexter mechanism involving electronic coupling between chromophores via the central aryl ring of the hexaphenylbenzene core evidently also contributes to the energy transfer process. Transfer from a BPEA meta to the porphyrin was found to be slower than transfer from a BPEA para to the porphyrin, even though Förster theory predicts meta transfer to be faster, due to the shorter interchromophore separation and comparable orientation factors. This may be ascribed to electron exchange transfer mediated by the chemical bonds joining the chromophores.

Electron Transfer. The free base porphyrin first excited singlet state, which has a lifetime of 10.3 ns in hexad **12**, lives only 2.0 ns in heptad **1** in 2-methyltetrahydrofuran. The quenching is due to formation of the $P^{\bullet+}-C_{60}^{\bullet-}$ charge-separated state, as demonstrated by the spectral data discussed above. The electron-transfer rate constant k_{CS} may be calculated according to eq 6, were τ is 2.0 ns and k_s is taken as the reciprocal of the 10.3 ns lifetime of the porphyrin first excited singlet state in **12**; k_{CS} equals 4.0×10^8 s^{-1}.

$$k_{CS} = (1/\tau) - k_s \qquad (6)$$

This rate constant is identical to that reported for a porphyrin−fullerene dyad with a structure similar to that of the porphyrin−fullerene portion of **1**.[48] The quantum yield of photoinduced electron transfer is 80%, whether light is absorbed in the antenna system or directly by the porphyrin moiety.

The lifetime of the charge separated state is 8.9 ns, giving a value for the rate constant for charge recombination, k_{CR}, of 1.1×10^8 s^{-1}. This rate constant is slightly smaller than that measured for the porphyrin−fullerene model system, 2.5×10^8 s^{-1}. The similarity of the two rate constants suggests that the radical cation of **1** in the charge-separated state most likely remains on the porphyrin, rather than migrating to the BPEA antenna moieties. This is reasonable on energetic grounds. The first oxidation potential of model BPEA system **4** was determined by cyclic voltammetry in benzonitrile solution containing 0.1 M tetra-*n*-butylammonium hexafluorophosphate, using a glassy carbon working electrode, platinum counter electrode, and $Ag/AgNO_3$ pseudo-reference electrode. Ferrocene was used as an internal standard. The oxidation potential for the model BPEA was 1.17 V vs SCE. That for a model for the porphyrin component of **1** is 1.03 V vs SCE.[57] Thus, migration of the positive charge into the antenna array would be endergonic.

The rate constant for photoinduced electron transfer in zinc heptad **2** is 1.2×10^{10} s^{-1}, and the lifetime of the charge-separated state is 15.3 ns. The quantum yield of charge separation is 96%. The zinc porphyrin moiety of **2** has a lower oxidation potential (0.76 V vs SCE)[57] than does the free base of **1** and a more energetic excited singlet state, leading to a larger thermodynamic driving force for photoinduced electron transfer and, therefore, a larger rate constant. The driving force

(53) Dirks, J. W.; Underwood, G.; Matheson, J. C.; Gust, D. *J. Org. Chem.* **1979**, *44*, 2551−2555.
(54) Gust, D.; Patton, A. *J. Am. Chem. Soc.* **1978**, *100*, 8175−8181.
(55) Braun, J.; Schlabach, M.; Wehrle, B.; Köcher, M.; Vogel, E.; Limbach, H. H. *J. Am. Chem. Soc.* **1994**, *116*, 6593−6604.
(56) Scholes, G. D. *Annu. Rev. Phys. Chem.* **2003**, *54*, 57−87.
(57) Gould, S. L.; Kodis, G.; Palacios, R. E.; de la Garza, L.; Brune, A.; Gust, D.; Moore, T. A.; Moore, A. L. *J. Phys. Chem. B* **2004**, *108*, 10566−10580.

for recombination of the charge-separated state of **2** to the ground state (1.35 eV) is consequently less than that for the corresponding state in **1** (1.62 eV). These recombination reactions are expected to occur in the Marcus inverted region,[58,59] where an increase in driving force leads to a decrease in rate. The opposite behavior is observed for **1** and **2**. This suggests that in one (or both) of the compounds, charge recombination in the normal Marcus region to yield triplet states may be occurring. Triplet states are indeed formed with **1** and, to a lesser extent, **2**, but we were not able to obtain definitive evidence for formation of triplets by charge recombination, rather than normal intersystem crossing.

Conclusions

Heptads **1** and **2** demonstrate efficient light harvesting by the five BPEA antenna moieties in the 430−480 nm spectral region. Solar irradiance is maximal in this spectral region, where porphyrins and chlorophylls are not very effective absorbers. The BPEA moieties of **1** and **2** fill the role of carotenoid polyenes, one of nature's primary antenna chromophores in this spectral region. Singlet energy transfer from the BPEA moieties to the porphyrin occurs on a surprisingly rapid time scale, a few picoseconds, and with a quantum yield of essentially unity. Hopping of excitation around the ring, between adjacent BPEA moieties, is the most rapid energy transfer process, although energy transfer from any of the BPEA units directly to the porphyrin also contributes to the overall process. The Förster dipole−dipole theory provides reasonable agreement with the experimental data. Once the excitation energy reaches the porphyrin moiety of **1** or **2**, photoinduced electron transfer occurs to produce a $P^{\bullet+}-C_{60}^{\bullet-}$ charge-separated state. The relatively slow electron transfer in free base **1** limits the quantum yield of charge separation to 80%. In the zinc analogue **2**, which features an increased thermodynamic driving force, the yield is 96%. Charge recombination occurs in 8.9 ns for **1** and 15.3 ns for **2**. The hexaphenylbenzene scaffold provides a rigid and versatile core for organizing antenna chromophores and coupling them efficiently to electron donor−acceptor systems, yielding functional analogues of natural photosynthetic antenna-reaction center complexes.

Acknowledgment. This work was supported by a grant from the U.S. Department of Energy (DE-FG02-03ER15393). J.A. is grateful to the Carl Trygger Foundation for Scientific Research for financial support. This is Publication No. 648 from the ASU Center for the Study of Early Events in Photosynthesis.

Supporting Information Available: Experimental details of the spectroscopic investigations. This material is available free of charge via the Internet at http://pubs.acs.org.

JA055903C

(58) Marcus, R. A. *J. Chem. Phys.* **1956**, *24*, 966−978.
(59) Marcus, R. A. *Pure Appl. Chem.* **1997**, *69*, 13−29.

Supporting Information

Energy and Photoinduced Electron Transfer in a Wheel-Shaped Artificial Photosynthetic Antenna-Reaction Center Complex

Gerdenis Kodis, Yuichi Terazono, Paul A. Liddell, Joakim Andréasson, Vikas Garg, Michael Hambourger, Thomas A. Moore, Ana L. Moore,* and Devens Gust**

Department of Chemistry and Biochemistry, Center for the Study of Early Events in Photosynthesis, Arizona State University, Tempe, AZ 85287-1604

E-mail: gust@asu.edu

Experimental Section

Steady-state spectroscopy. The solvent for all spectroscopic measurements was freshly distilled 2-methyltetrahydrofuran, unless otherwise stated. Ground state absorption spectra were measured on a Shimadzu UV-3101PC UV-vis-NIR spectrometer. Steady state fluorescence emission spectra were measured using a Photon Technology International MP-1 fluorometer and corrected. Excitation was produced by a 75 W xenon lamp and single grating monochromator. Fluorescence was detected at 90° to the excitation beam via a single grating monochromator and an R928 photomultiplier tube having S-20 spectral response operating in the single-photon-counting mode.

Time-resolved fluorescence. Fluorescence decay measurements were performed on ~1×10^{-5} M solutions by the single photon timing method. The excitation source was a cavity-dumped Coherent 700 dye laser pumped by a frequency-doubled Coherent Antares 76s Nd:YAG laser.

Fluorescence emission was detected at a magic angle using a double grating monochromator and microchannel plate photomultiplier (Hamamatsu R2809U-11). The instrument response time was *ca.* 40-120 ps, as verified by scattering from Ludox AS-40 at the excitation wavelength.[1] Fluorescence anisotropy decays were obtained by changing the detection polarization of the fluorescence path parallel or perpendicular to the polarization of the excitation light. The anisotropy decays then were calculated according to eq. 1, where $I_{VV}(t)$ (or $I_{VH}(t)$) is the fluorescence decay when the excitation light is vertically polarized and only the vertically (or horizontally) polarized portion of fluorescence is detected, denoting that the first and second subscripts represent excitation and detection polarization, respectively. The factor G which is equal to the ratio of the sensitivities of the detection system for vertically and horizontally polarized light can be determined either by so-called tail matching of $I_{VV}(t)$ and $I_{VH}(t)$ or by $I_{HV}(t)/I_{HH}(t)$.

Nanosecond transient absorption. Nanosecond transient absorption measurements were made with excitation from an OPOTEK optical parametric oscillator driven by the third harmonic of a Continuum Surelight Nd:YAG laser. The pulse width was ~4-5 ns, and the repetition rate was 10 Hz. The detection portion of the spectrometer was manufactured by Ultrafast Systems.

Subpicosecond transient absorption. The femtosecond transient absorption apparatus consisted of a kilohertz pulsed laser source and a pump-probe optical setup. The laser pulse train was provided by a Ti:Sapphire regenerative amplifier (Clark-MXR, Model CPA-1000) pumped by a diode-pumped CW solid state laser (Spectra Physics, Model Millennia V). The typical laser pulse was 100 fs at 790 nm, with a pulse energy of 0.9 mJ at a repetition rate of 1 KHz. Most of the laser energy (80%) was used to pump an optical parametric amplifier (IR-OPA, Clark-MXR).

The excitation pulse was sent through a computer-controlled optical delay line. The remaining laser output (20%) was focused onto a flowing water cell to generate a white-light continuum. The continuum beam was further split into two identical parts and used as the probe and reference beams, respectively. The probe and reference signals were focused onto two separated optical fiber bundles coupled to a spectrograph (Acton Research, Model SP275). The spectra were acquired on a dual diode array detector (Princeton Instruments, Model DPDA-1024).[2]

For the transient absorption anisotropy decay ($r(t)$) measurements another kilohertz pulsed laser source and a pump-probe optical setup were employed. Laser pulses of 100 fs at 800 nm were generated by an amplified, mode-locked Titanium Sapphire kilohertz laser system (Millennia/Tsunami/Spitfire, Spectra Physics). Part of the laser pulse energy was sent through an optical delay line and focused on a 2 mm sapphire plate to generate a white light continuum for the probe beam. The remainder of the pulse energy was used to pump an optical parametric amplifier (Spectra Physics) to generate excitation pulses, which were modulated using a mechanical chopper. The excitation intensity was adjusted using a continuously variable neutral density filter. The probe beam was sent through a monochromator (SP150, Action Res. Corp.) and recorded by a diode detector (Model 2032, New Focus Inc.) and box car (SR250, Stanford Research Systems). The excitation pulse was adjusted to have parallel or perpendicular polarization with respect to the polarization of the probe pulse by rotating a broadband half wave plate. Finally, the transient absorption anisotropy decay was obtained from eq. 7, where A is the signal amplitude.

$$r(t) = \frac{\Delta A_{VV}(t) - \Delta A_{HV}(t)}{\Delta A_{VV}(t) + 2\Delta A_{HV}(t)} \tag{7}$$

To determine the number of significant components in the transient absorption data, singular value decomposition analysis[3,4] was carried out using locally-written software

(ASUFIT) developed under a MATLAB environment (Mathworks Inc.). Decay-associated spectra were then obtained by fitting the transient absorption change curves over a selected wavelength region simultaneously as described by Equation 8,

$$\Delta A(\lambda,t) = \sum_{i=1}^{n} A_i(\lambda)\exp(-t/\tau_i) \qquad (8)$$

where $\Delta A(\lambda,t)$ is the observed absorption change at a given wavelength at time delay t and n is the number of kinetic components used in the fitting. A plot of $A_i(\lambda)$ versus wavelength is called a decay-associated spectrum, and represents the amplitude spectrum of the i^{th} kinetic component, which has a lifetime of τ_i.

Random errors associated with the reported lifetimes obtained from fluorescence and transient absorption measurements were typically <10% judging from the standard deviation of fitting parameters and results obtained from analysis of different data sets taken over similar spectral ranges.

References

(1) Gust, D.; Moore, T. A.; Luttrull, D. K.; Seely, G. R.; Bittersmann, E.; Bensasson, R. V.; Rougée, M.; Land, E. J.; de Schryver, F. C.; Van der Auweraer, M. *Photochem. Photobiol.* **1990**, *51*, 419-426.

(2) Freiberg, A.; Timpmann, K.; Lin, S.; Woodbury, N. W. *J. Phys. Chem. B* **1998**, *102*, 10974-10982.

(3) Golub, G. H.; Reinsch, C. *Numer. Math.* **1970**, *14*, 403-420.

(4) Henry, E. R.; Hofrichter, J. *Methods in Enzymology* **1992**, *210*, 129-192.